



# Electronic transport for polymer/Si-nanowire arrays/n-type Si diodes with and without Si-nanowire surface passivation

Wei-Min Cho<sup>a</sup>, Yow-Jon Lin<sup>a,\*</sup>, Hsing-Cheng Chang<sup>b</sup>, Ya-Hui Chen<sup>c</sup>

<sup>a</sup> Institute of Photonics, National Changhua University of Education, Changhua 500, Taiwan

<sup>b</sup> Department of Automatic Control Engineering, Feng Chia University, Taichung 407, Taiwan

<sup>c</sup> Precision Instrument Support Center, Feng Chia University, Taichung 407, Taiwan

## ARTICLE INFO

### Article history:

Received 18 November 2012

Received in revised form 9 February 2013

Accepted 14 March 2013

Available online 26 March 2013

### Keywords:

Si

Diode

Electrical property

Defect

Nanostructure

## ABSTRACT

The effect of Si-nanowire (SiNW) surface passivation on electronic transport of heterojunction diodes based on the poly(3,4-ethylenedioxythiophene) doped with poly(4-styrenesulfonate) (PEDOT:PSS) and n-type Si with SiNW arrays was investigated in this study. The PEDOT:PSS/SiNWs/n-type Si diode without SiNW surface passivation shows a poor rectifying behavior with an ideality factor ( $\eta$ ) of 7.8 and high leakage. However, the PEDOT:PSS/SiNWs/n-type Si diode with SiNW surface passivation shows a good rectifying behavior with  $\eta$  of 1.7 and low leakage. Such an improvement indicates that a good passivation is formed at the interface as a result of a combined effect of the formation of Si–O bonds and the removal of the short-lifetime charge traps. Note that SiNW surface passivation plays a significant role in the photoconduction by providing the contribution of long-lifetime charge trapping to the decay process.

© 2013 Elsevier B.V. All rights reserved.

## 1. Introduction

Hybrid organic–inorganic electronics has been a subject of extensive research [1–12]. The use of heterostructures is an effective way of manipulating the electronic and optoelectronic properties of devices. But a precise control on the junction properties like the built-in electrical potential and ideality factor ( $\eta$ ) cannot be done due to the presence of interface defects. Thus interface passivation is crucial in order to fabricate a stable and reliable device. Hybrid organic–inorganic devices are commonly made of p-type organic semiconductors combined with n-type Si (n-Si) structures [5–12]. Among many conductive polymers, the beneficial properties of poly(3,4-ethylenedioxythiophene) doped with poly(4-styrenesulfonate) (PEDOT:PSS), such as high transparency and environmental robustness, have attracted significant interest for application in optoelectronic devices [5–12]. Hybrid solar cells fabricated by spin coating PEDOT:PSS on planar Si and Si-nanowire (SiNW) arrays have reported by Lu et al. [9] and He et al. [11]. The high efficiency and simple solution process used suggest that such devices are promising for developing low cost and high efficiency SiNWs/organic solar cells. However, SiNW arrays add complexity to the device design and fabrication due to surface states and surface recombination [7]. Therefore, the work on SiNW surface passivation is needed to control the interfacial recombination

mechanisms, in order to optimize charge separation and collection efficiencies in nanowire junction devices. In this work, we demonstrated hybrid p–n diodes based on the PEDOT:PSS and n-type Si (n-Si) with SiNW arrays (denoted PEDOT:PSS/SiNWs/n-Si). A simple passivation technique (that is,  $\text{H}_2\text{O}_2$  treatment) to find the effect of SiNW surface passivation on electronic transport for PEDOT:PSS/SiNWs/n-Si diodes was developed in this study. It is shown a good rectifying behavior by adopting a simple and inexpensive chemical route. We found that the interfacial defects of the PEDOT:PSS/SiNWs/n-Si diode were controlled by  $\text{H}_2\text{O}_2$  treatment, improving the device performance.

## 2. Experimental

Four-inch n-Si (100) wafers purchased from Woodruff Tech Company (U.S.A.) were used in the experiment. The 525- $\mu\text{m}$  thick n-Si wafers were doped with phosphorus to about  $2 \times 10^{15} \text{ cm}^{-3}$ . The n-Si samples were cleaned in chemical cleaning solutions of acetone and methanol, rinsed with de-ionized water, and blow-dried with  $\text{N}_2$ . Next, the n-Si sample was chemically etched with a diluted HF solution for 1 min, rinsed with de-ionized water and blow-dried with  $\text{N}_2$ . The SiNWs arrays were then formed adopting a developed silver-induced wet-chemical-etching process in an aqueous buffered HF and  $\text{AgNO}_3$  etching solution at 25 °C [7]. The etching time was 15 min. The surface color of these wafers appeared black after removing the Ag remnants by immersing them in the concentrated  $\text{HNO}_3$  solution for one hour. The length

\* Corresponding author. Tel.: +886 4 7232105/3379; fax: +886 4 7211153.

E-mail address: [rzr2390@yahoo.com.tw](mailto:rzr2390@yahoo.com.tw) (Y.-J. Lin).

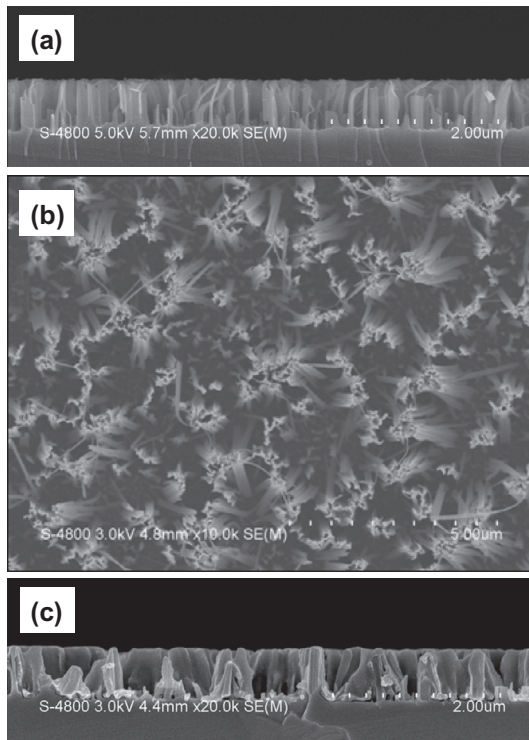


**Fig. 1.** (a) Cross-sectional and (b) plane SEM images of the SiNWs and (c) cross-sectional image of the PEDOT:PSS/SiNWs/n-Si sample.

of SiNWs, as estimated from field emission scanning electron microscopy (SEM), was  $535 \pm 5$  nm. Fig. 1 shows cross-sectional and plane SEM images of the SiNWs. Then, some of the SiNWs/n-Si samples were dipped in the  $\text{H}_2\text{O}_2$  solution at  $60^\circ\text{C}$  for 10 min (referred to as  $\text{H}_2\text{O}_2$ -treated SiNWs/n-Si samples). Then, PEDOT:PSS (Clevios P VP, Al 4083) purchased from Heraeus was deposited on SiNWs/n-Si samples with and without  $\text{H}_2\text{O}_2$  treatment by spin coating, respectively. Spin casting was performed at 1500 rpm for 60 s per cast layer. After depositing by spin coating, the films were baked at  $150^\circ\text{C}$  for 30 min on a hotplate. The procedures from coating to drying were repeated seven times. Fig. 1(c) shows the cross-sectional SEM image of the PEDOT:PSS/SiNWs/n-Si sample. The thickness of the PEDOT:PSS layer, as estimated from SEM, was  $590 \pm 5$  nm. In (80 nm) ohmic contacts were deposited onto the back surface of n-Si by a sputter coater. In addition, Au (100 nm) ohmic contacts were deposited onto the PEDOT:PSS surface. Au electrodes with interdigitated patterns were produced using shadow masking through sputter coater. The area over which the SiNWs were formed is  $30 \times 30 \text{ mm}^2$ . Nine diodes were made from a SiNW sample. The area of a diode is  $5 \times 5 \text{ mm}^2$ . The fabricated devices were placed in a nitrogen-filled glove box. The current–voltage ( $I$ – $V$ ) and current–time ( $I$ – $t$ ) curves were measured using a Keithley Model-4200-SCS semiconductor characterization system. The photoreponse was measured under  $100 \text{ mW/cm}^2$  and illumination intensity from a 150 W solar simulator with an AM 1.5 G filter (obtained from Newport Corporation). The photoreponse was measured by recording the current versus time while sunlight illumination was turned on and off by a shutter. To understand the improved device performance for  $\text{H}_2\text{O}_2$ -treated samples, the Si 2p core levels of the SiNWs/n-Si surfaces with and without  $\text{H}_2\text{O}_2$  treatment were analyzed using X-ray photoelectron spectroscopy (XPS). XPS measurements were performed using a monochromatic Al  $K\alpha$  X-ray source. We took an Au 4f peak and a C 1s peak for energy reference purposes.

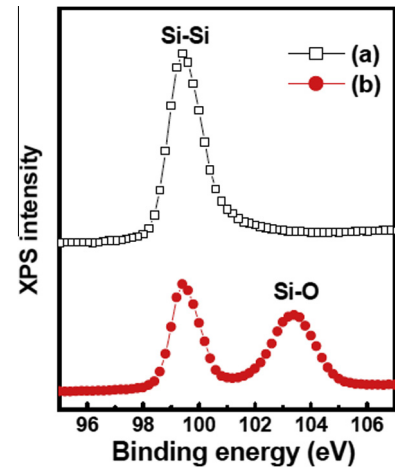


**Fig. 2.** Si 2p core-level spectra at the SiNWs/n-Si surfaces (a) without and (b) with  $\text{H}_2\text{O}_2$  treatment.

### 3. Results and discussion

Fig. 2 shows the Si 2p core-level spectra of SiNWs/n-Si samples with and without  $\text{H}_2\text{O}_2$  treatment. The peak positioned at 99.4 eV is attributed to Si–Si bonds and the peak positioned at 103.3 eV is attributed to Si–O bonds [13,14]. The Si–O bonds were found at the  $\text{H}_2\text{O}_2$ -treated SiNWs/n-Si surfaces. Malik et al. [15] and He and Lin [13] found that an ultra thin  $\text{SiO}_x$  layer was grown on the n-Si surface by immersing the wafer in a  $\text{H}_2\text{O}_2$  solution during 10 min.

Fig. 3 shows the  $I$ – $V$  characteristics of the PEDOT:PSS/SiNWs/n-Si and PEDOT:PSS/ $\text{H}_2\text{O}_2$ -treated SiNWs/n-Si diodes in the dark, respectively. The rectifying  $I$ – $V$  characteristics suggest that Schottky junctions are formed at the PEDOT:PSS/SiNWs/n-Si and PEDOT:PSS/ $\text{H}_2\text{O}_2$ -treated SiNWs/n-Si interfaces. The ratio of the forward to reverse current at a bias voltage of  $\pm 1$  V for the PEDOT:PSS/SiNWs/n-Si (PEDOT:PSS/ $\text{H}_2\text{O}_2$ -treated SiNWs/n-Si) diode was calculated to be 2 (207), implying a poor (good) rectification behavior for PEDOT:PSS/SiNWs/n-Si (PEDOT:PSS/ $\text{H}_2\text{O}_2$ -treated SiNWs/n-Si) diodes. The conduction mechanism in a p–n diode usually follows the thermionic emission. The behavior under high-forward bias may be suggestive of the domination of the series resistance ( $R_s$ ). It is found that  $\text{H}_2\text{O}_2$  treatment may lead to increased current at high-forward voltage, implying that  $R_s$  of the PEDOT:PSS/ $\text{H}_2\text{O}_2$ -treated SiNWs/n-Si diode is lower than that of the PEDOT:PSS/SiNWs/n-Si diode. In addition,  $\eta$  was determined from the slope of the linear regions of the forward-bias  $I$ – $V$  plots.

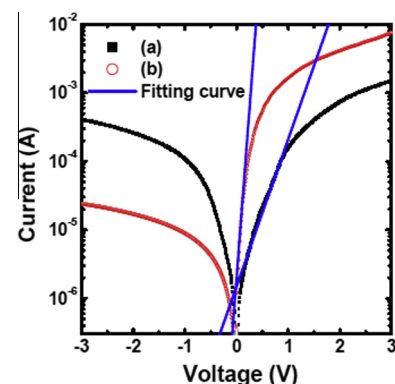


**Fig. 3.**  $I$ – $V$  curves of (a) PEDOT:PSS/SiNWs/n-Si and (b) PEDOT:PSS/ $\text{H}_2\text{O}_2$ -treated SiNWs/n-Si diodes in the dark.

From the curve fitting of  $I$ – $V$  characteristic of the PEDOT:PSS/SiNWs/n-Si (PEDOT:PSS/H<sub>2</sub>O<sub>2</sub>-treated SiNWs/n-Si) diode,  $\eta$  of 7.8 (1.7) was extracted. There were nine diodes per substrate and the variation in  $\eta$  of the working diodes was within 10%. The reported  $\eta$  of the PEDOT:PSS/H<sub>2</sub>O<sub>2</sub>-treated SiNWs/n-Si diode here is smaller than previously published values for PEDOT:PSS/SiNWs devices [16,17]. This high value of  $\eta$  (that is,  $\eta > 2$ ) suggests that the  $I$ – $V$  characteristic of our PEDOT:PSS/SiNWs/n-Si diode is not limited by the forward-bias current behavior of the conventional p–n junction. Deviation of  $\eta$  from unity may be attributed to either the recombination of electrons and holes in the depletion region and/or presence of a large number of the interfacial defects [18,19]. Maeng et al. found  $\eta$  of 96 extracted for the PEDOT:PSS/ZnO nanowall network heterojunction diode, indicating that the charge traps influence the electronic conduction through the device [20]. However, this PEDOT:PSS/H<sub>2</sub>O<sub>2</sub>-treated SiNWs/n-Si diode shows a good rectifying behavior with  $\eta$  of 1.7. We suggested that the interfacial defects may play important roles in the conduction process of the PEDOT:PSS/SiNWs/n-Si diode. In addition, as compared to PEDOT:PSS/SiNWs/n-Si diodes, the leakage current is significantly decreased by about 15 times for PEDOT:PSS/H<sub>2</sub>O<sub>2</sub>-treated SiNWs/n-Si diodes. A probable reason for the large leakage current is the existence of the high interfacial defect density. According to the reported result by Umeda et al. [21], leakage currents are dominated by generation-recombination currents, which are due to defects. Such an improvement indicates that a good passivation is formed at the interface as a result of the reduction of the interfacial defect density and an appropriate interfacial SiO<sub>x</sub> layer plays an important role in the conduction process of a hybrid p–n diode.

To further examine the effect of H<sub>2</sub>O<sub>2</sub> treatment on the electrical characteristics of PEDOT:PSS, the photoresponse of the PEDOT:PSS/SiNWs/n-Si or PEDOT:PSS/H<sub>2</sub>O<sub>2</sub>-treated SiNWs/n-Si diode was measured. Fig. 4 shows the time-resolved response of the current to repeated light switching with cycling times between 0 and 300 s for  $V$  varying from 0 to 1  $\mu$ V. A negative photocurrent ( $I_p$ ) is found for  $V$  varying from 0 to 1  $\mu$ V, implying that the PEDOT:PSS/SiNWs/n-Si (or PEDOT:PSS/H<sub>2</sub>O<sub>2</sub>-treated SiNWs/n-Si) depletion region contributes to the photoresponse.  $I_p$  gives the current at near zero voltage and nearly equals the short circuit current. We found that the time-dependent  $I_p$  is strongly affected upon H<sub>2</sub>O<sub>2</sub> treatment. Compared to a PEDOT:PSS/SiNWs/n-Si device, the PED-

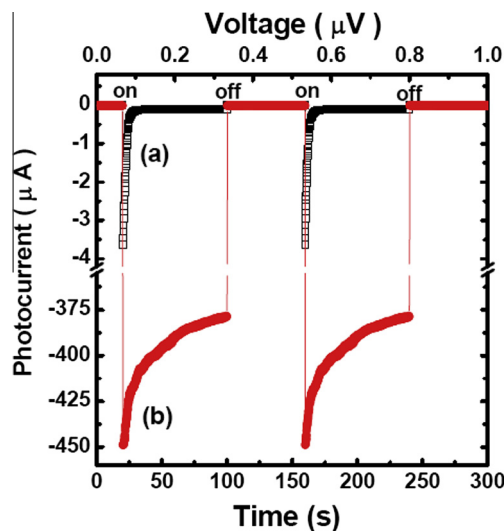


**Fig. 4.** Time-resolved photocurrent measurements for (a) PEDOT:PSS/SiNWs/n-Si and (b) PEDOT:PSS/H<sub>2</sub>O<sub>2</sub>-treated SiNWs/n-Si diodes (on and off switching of sunlight illumination is indicated).

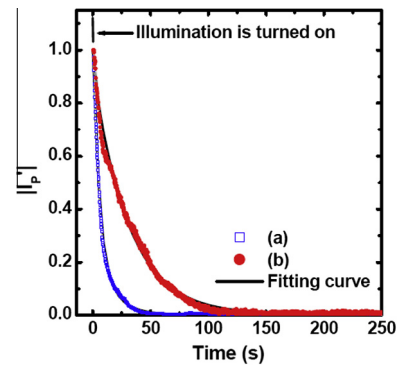


**Fig. 5.** The normalized photocurrent ( $|I_p|$ ) decay for (a) PEDOT:PSS/SiNWs/n-Si and (b) PEDOT:PSS/H<sub>2</sub>O<sub>2</sub>-treated SiNWs/n-Si diodes.

OT:PSS/H<sub>2</sub>O<sub>2</sub>-treated SiNWs/n-Si diode showed much greater  $|I_p|$ . This PEDOT:PSS/H<sub>2</sub>O<sub>2</sub>-treated SiNWs/n-Si diode shows a good rectifying behavior with  $\eta$  of 1.7, low leakage and low  $R_s$ , implying that the increased photocurrent may be related to the improved rectifying  $I$ – $V$  characteristics of the diodes. In addition,  $|I_p|$  should rapidly decay for PEDOT:PSS/SiNWs/n-Si diodes, since the charge traps at the PEDOT:PSS/SiNWs/n-Si interface influence the electronic conduction through the device. However,  $|I_p|$  should slowly decay for PEDOT:PSS/H<sub>2</sub>O<sub>2</sub>-treated SiNWs/n-Si diodes, indicating that H<sub>2</sub>O<sub>2</sub> treatment may lead  $I_p$  stability improvement.

To confirm these pictures, time domain measurement was performed on the PEDOT:PSS/SiNWs/n-Si or PEDOT:PSS/H<sub>2</sub>O<sub>2</sub>-treated SiNWs/n-Si diode. The  $I_p$  values were measured for  $V$  varying from 0 to 1  $\mu$ V for 250 s (Illumination was turned on at  $t = 0$  s). Fig. 5 shows the normalized  $|I_p|$  decay for PEDOT:PSS/SiNWs/n-Si and PEDOT:PSS/H<sub>2</sub>O<sub>2</sub>-treated SiNWs/n-Si diodes, respectively. In this study, we consider two possible physical pictures to explain the observed  $I_p$  characteristic: It is mainly dominated by the interfacial long-lifetime or short-lifetime charge traps. To estimate the time constants for  $|I_p|$  decay, we fit the data to exponential decay functions. The transient was fitted to second-order exponential decay  $|I_p| = A_1 e^{-(t/\tau_1)} + A_2 e^{-(t/\tau_2)}$  using the nonlinear least-squares method [6,22,23], with four fitting parameters, as listed in Table 1.  $|I_p|$  is the normalized  $|I_p|$ . This equation reflects two different charge trapping mechanisms with time constants  $\tau_1$  and  $\tau_2$  ( $\tau_1 > \tau_2$ ). The values of  $A_1$  and  $A_2$ , where  $A_1 + A_2 = 1$ , represent weighing factors that quantify the contribution of each mechanism to the decay process. The first (second) term, which can be attributed to long-lifetime (short-lifetime) charge trapping, dominates the decay process. For the PEDOT:PSS/SiNWs/n-Si diode, the data show that  $|I_p|$  rapidly decayed, owing to a large number of the interfacial defects and the domination of short-lifetime charge trapping ( $A_1 < A_2$ ). However,  $|I_p|$  slowly decayed for the PEDOT:PSS/H<sub>2</sub>O<sub>2</sub>-treated SiNWs/n-Si diode, owing to the removal of the short-lifetime charge traps (that is,  $A_2 = 0$ ) and the domination of long-lifetime charge trapping. Note that H<sub>2</sub>O<sub>2</sub> treatment plays a significant role in the photoconduction by providing the contribution of long-lifetime charge trapping to the decay process. In addition, we found that H<sub>2</sub>O<sub>2</sub> treatment may lead to an increase in  $\tau_1$ , resulting in the stability improvement of  $I_p$ . High responsivity thus originates from efficient carrier transport combined with long-lifetime charge trapping. An

**Table 1**  
Fitting parameters and results.

	$\tau_1$ (s)	$A_1$	$\tau_2$ (s)	$A_2$
PEDOT:PSS/SiNWs/n-Si	13.8	0.31	4.5	0.69
PEDOT:PSS/H <sub>2</sub> O <sub>2</sub> -treated SiNWs/n-Si	30.8	1	x	x

exhibition of high quantum efficiency of the PEDOT:PSS/H<sub>2</sub>O<sub>2</sub>-treated SiNWs/n-Si diode is attributed to a combined effect of the formation of Si–O bonds and the removal of the short-lifetime charge traps. Due to the heterojunction nature, the interface is very important and can easily form defects that can diminish the device performance [24].

#### 4. Conclusions

In summary, we have discussed the fabrication and electrical properties of heterojunction diodes based on the PEDOT:PSS and n-Si with SiNW arrays. The PEDOT:PSS/SiNWs/n-Si diode shows a poor rectifying behavior with  $\eta$  of 7.8 and high leakage, implying that the interfacial defects influence the electronic conduction through the device. However, the PEDOT:PSS/H<sub>2</sub>O<sub>2</sub>-treated SiNWs/n-Si diode shows a good rectifying behavior with  $\eta$  of 1.7 and low leakage. Such an improvement indicates that a good passivation is formed at the interface as a result of the removal of the short-lifetime charge traps and the formation of Si–O bonds. These experimental demonstrations suggest that it may be possible to minimize the adverse effects of the interfacial defects to obtain functional devices using H<sub>2</sub>O<sub>2</sub> treatment.

#### Acknowledgments

The authors acknowledge the support of the National Science Council of Taiwan (Contract no. 101-2120-M-194-002) in the form of grants.

#### References

- [1] Y.J. Lin, C.F. You, C.Y. Chuang, *ECS J. Solid State Sci. Technol.* 2 (2013) Q31.
- [2] Y.J. Lin, T.H. Su, J.C. Lin, Y.C. Su, *Synth. Met.* 162 (2012) 406.
- [3] Y.R. Park, Y.J. Lee, C.J. Yu, J.H. Kim, *J. Appl. Phys.* 108 (2010) 044508.
- [4] J.J. Zeng, C.L. Tsai, Y.J. Lin, *Synth. Met.* 162 (2012) 1411.
- [5] Y.J. Lin, Y.C. Su, *J. Appl. Phys.* 111 (2012) 073712.
- [6] J.H. Lin, J.J. Zeng, Y.C. Su, Y.J. Lin, *Appl. Phys. Lett.* 100 (2012) 153509.
- [7] H. Li, R. Jia, C. Chen, Z. Xing, W. Ding, Y. Meng, D. Wu, X. Liu, T. Ye, *Appl. Phys. Lett.* 98 (2011) 151116.
- [8] T.G. Chen, B.Y. Huang, E.C. Chen, P. Yu, H.F. Meng, *Appl. Phys. Lett.* 101 (2012) 033301.
- [9] W. Lu, Q. Chen, B. Wang, L. Chen, *Appl. Phys. Lett.* 100 (2012) 023112.
- [10] L. He, C. Jiang, Rusli, D. Lai, H. Wang, *Appl. Phys. Lett.* 99 (2011) 021104.
- [11] L. He, C. Jiang, H. Wang, D. Lai, Y.H. Tan, C.S. Tan, Rusli, *Appl. Phys. Lett.* 100 (2012) 103104.
- [12] H.C. Neitzert, S. Schwertheim, K. Meusinger, M. Leinhos, W.R. Fahrner, *Proc. SPIE* 7364 (2009) 73640L, <http://dx.doi.org/10.1117/12.821469>.
- [13] G.R. He, Y.J. Lin, *Mater. Chem. Phys.* 136 (2012) 179.
- [14] R. Alfonsetti, L. Lozzi, M. Passacantando, P. Picozzi, S. Santucci, *Appl. Surf. Sci.* 70 (1993) 222.
- [15] O. Malik, F.J. De la Hida-W, C. Zúñiga-I, G. Ruiz-T, J. Non-Crystalline Solids 354 (2008) 2472.
- [16] W. Lu, C. Wang, W. Yue, L. Chen, *Nanoscale* 3 (2011) 3631.
- [17] S.A. Moiz1, A.M. Nahhas, H.D. Um, S.W. Jee, H.K. Cho, S.W. Kim, J.H. Lee, *Nanotechnology* 23 (2012) 145401.
- [18] M. Campos, L.O.S. Bulhoes, C.A. Lindino, *Sens. Actuators* 87 (2000) 67.
- [19] F. Yakuphanoglu, *Synth. Met.* 157 (2007) 859.
- [20] J. Maeng, M. Jo, S.J. Kang, M.K. Kwon, G. Jo, T.W. Kim, J. Seo, H. Hwang, D.Y. Kim, S.J. Park, T. Lee, *Appl. Phys. Lett.* 93 (2008) 123109.
- [21] T. Umeda, A. Toda, Y. Mochizuki, *Eur. Phys. J. Appl. Phys.* 27 (2004) 13.
- [22] G. Gu, M.G. Kane, J.E. Doty, A.H. Firester, *Appl. Phys. Lett.* 87 (2005) 243512.
- [23] B.C. Huang, Y.J. Lin, *Appl. Phys. Lett.* 99 (2011) 113301.
- [24] P.T. Mersich, T. Yen, A. Anderson, in: 34th IEEE Photovoltaic Specialists Conference, 2009, p. 000390.